

# Recent Results from the PHENIX Experiment at RHIC

J. Lajoie<sup>a</sup> for the PHENIX Collaboration

<sup>a</sup> Department of Physics and Astronomy, Iowa State University,  
Ames, Iowa 50011

The PHENIX experiment has been designed to measure a wide variety of observables in both heavy ion and polarized proton collisions at RHIC. The use of penetrating probes of the earliest stages of the collision, combined with a program of hadron measurements, gives the experiment the capability to address observables sensitive to all stages of a heavy ion collision. This contribution will review recent results from the PHENIX collaboration for heavy-ion collisions, including hadronic spectra, collective motion of the interacting matter, the suppression of high transverse momentum hadrons, and charm production.

## 1. Introduction

The primary goals of the PHENIX experimental program [1] at the Relativistic Heavy Ion Collider (RHIC) are the detection of the quark-gluon plasma (QGP) and subsequent characterization of its properties. The PHENIX collaboration plans to investigate the physics of the QGP [2] with a broad-based physics program using a variety of observables. Establishing the existence of the QGP and studying its properties will require the correlation of many experimental measurements. The PHENIX experiment is designed with a broad physics program in mind and is capable of measuring leptons, photons, and hadrons with excellent energy and momentum resolution. The use of lepton probes of the QGP in particular allows a window into the heavy-ion collision that is unperturbed by final state interactions.

## 2. The PHENIX Experiment

The PHENIX detector consists of a set of global event detectors and four spectrometer arms, with each pair of spectrometer arms dedicated to a specific set of physics measurements. A pair of spectrometers measuring electrons, photons and hadrons covers mid-rapidity, while a second pair of spectrometers measures muons at forward rapidities. The magnetic field in the collision region of the PHENIX detector is axial, while the magnets of the muon arms produce a radial field. Overall the PHENIX detector will consist of eleven independent subsystems working together in an integrated manner, using a variety of technologies to provide very discriminating particle identification capabilities.

In the inner portion of the PHENIX detector, closest to the interaction region, are the detectors used for global event characterization. Both the Multiplicity and Vertex Detector (MVD) and Beam Beam counters (BB) measure the interaction vertex and provide

information about the charge particle flux from an interaction. The central spectrometer arms (referred to as “East” and “West”) measure electron and hadron production near central rapidity using a variety of tracking detectors (drift chambers and pad chambers in both arms, and a time expansion chamber in the East arm) and particle identification detectors (ring imaging cerenkov counters in both arms, and a time-of-flight panel in the East arm). Both arms end in electromagnetic calorimeters (EMCAL, a combination of Pb-scintillator and Pb-glass detectors) that allow for measurements of photons and neutral pions, as well as provide global event characterization through transverse energy. Finally, the two muon arms (referred to as “North” and “South”) contain three stations of cathode strip tracking chambers followed by panels of Iarocci streamer tubes alternating with plates of steel absorber for muon identification.

### 3. Hadronic Observables

Measurements of hadrons originating from heavy-ion collisions carry information about the final state of the collision system and the freeze-out of the hadronic degrees of freedom. This final state information can often be used to infer the conditions of the system at an earlier time. For example, measurements of the transverse energy as a function of pseudorapidity ( $dE_T/d\eta$ ) can be combined with a Bjorken model of a hydrodynamically expanding source to infer that the energy density created in Au+Au collisions at RHIC is greater than  $4\text{-}5 \text{ GeV}/fm^3$  [3]. In addition, measurements of the transverse momentum distribution of identified hadrons show a rise in the mean transverse momentum as a function of particle mass [4]. This is characteristic of a hydrodynamically expanding system in which the particles are boosted by a velocity field, which translates to a larger transverse momentum kick for larger mass. By simultaneously fitting the particle spectra to a common freeze-out temperature and transverse flow velocity profile we obtain a freeze-out temperature of  $T_{fo} = 110 \pm 23 \text{ MeV}$  and transverse flow velocity of  $\beta_T = 0.7 \pm 0.2$  for the 10% most central  $\sqrt{s_{NN}} = 200 \text{ GeV}$  data [5]. This large freeze-out velocity indicates that the system has developed significant pressure during the collision.

#### 3.1. Elliptic Flow

Having observed that the colliding system develops a significant flow velocity, we can attempt to further characterize the system by investigating the azimuthal anisotropy of the produced particles. This is done by making a Fourier decomposition of the observed particle spectra and characterizing the distribution of particles by the second order coefficient of the expansion, called  $v_2$ . This approach is motivated by the fact that for non-central collisions the nuclear overlap is an almond shaped region that is elongated out of the interaction plane defined by the impact parameter between the two nuclei. If the system develops significant pressure due to the interaction of the matter in the overlap region, the pressure gradient will be larger in the direction of the interaction plane due to the anisotropic shape of the overlap region. This pressure gradient will convert the initial position space anisotropy of the system to a momentum space anisotropy in the final state.

For almost all particles produced in the collision ( $p_T < 2.5 \text{ GeV}/c$ ), the observed  $v_2$  is consistent with a hydrodynamic expansion of the colliding system coupled with the anisotropic initial overlap of the two nuclei [5]. The matter in this low momentum region

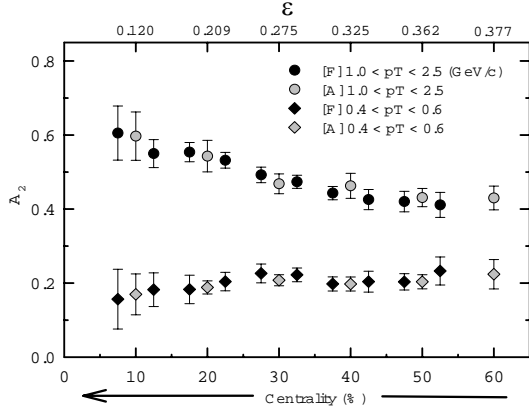


Figure 1. The scaled elliptic flow parameter  $A_2$  versus centrality and eccentricity of the colliding system, for Au+Au collisions at  $\sqrt{s_{NN}} = 130$  GeV. The different symbols for each momentum range indicate the results of two different methods for binning the particles as a function of momentum in generating the distributions used for the Fourier analysis.

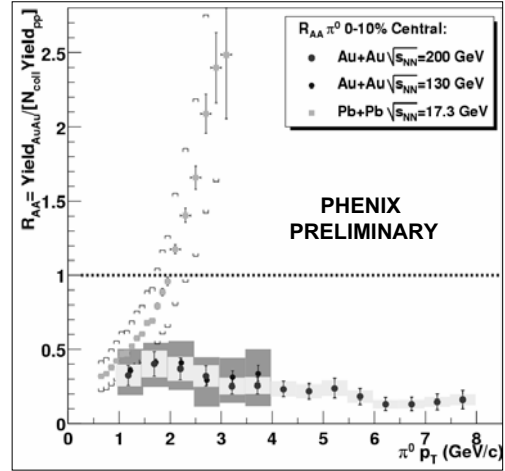


Figure 2. The nuclear modification factor  $R_{AA}$  for neutral pions in central collisions measured in the PHENIX apparatus, for both  $\sqrt{s_{NN}} = 130$  GeV and  $\sqrt{s_{NN}} = 200$  GeV collisions. Data from the CERN SPS is also shown, where initial state parton scattering dominates energy loss, producing an enhancement in the  $R_{AA}$  ratio above 2 GeV/c. The error bars on the PHENIX data are statistical, while the shaded bands indicate the systematic error.

is dominated by soft, non-perturbative QCD interactions and participates fully in the hydrodynamic expansion. One way to study this is to divide the elliptic flow parameter by the eccentricity of the collision,  $\epsilon = \langle y^2 \rangle - \langle x^2 \rangle / \langle y^2 \rangle + \langle x^2 \rangle$ , to yield a parameter known as the scaled elliptic flow,  $A_2 = v_2/\epsilon$ . In principle, the scaled elliptic flow should remove the geometric dependence of  $v_2$  on the shape of the nuclear overlap, allowing us to study the scaling of the elliptic flow as a function of the centrality of the collision.

The scaled elliptic flow observed by PHENIX in  $\sqrt{s_{NN}} = 130$  GeV Au+Au collisions is shown in Figure 1. Note that while the scaled elliptic flow is essentially flat for a low momentum sample of particles, the high momentum region shows a change in the scaled elliptic flow as a function of the centrality of the collision. For the high momentum particle sample a large fraction of the particles come from hard scattering interactions in the early stage of the collision. The behavior of the scaled elliptic flow for these particles may be an indication that the scattered partons suffer energy loss in traversing the dense medium. This energy loss combined with the anisotropic shape of the nuclear overlap region would induce a nonzero  $v_2$  parameter for these high momentum particles [6].

## 4. Hard Scattering

As indicated in the previous section, hard scattering between partons in the early stages of the collision can in principle provide an excellent probe of the matter produced in a heavy-ion collision. Hard scattered partons must traverse a dense, gluon-rich medium before hadronizing and can lose a significant fraction of their energy to gluon radiation. This is predicted to be observed as a suppression of hadrons at high transverse momentum [7].

The PHENIX detector is capable of reconstructing the decay of the  $\pi^0$  meson to two photons using the electromagnetic calorimeter in both central arms. Using the measured production of  $\pi^0$  mesons in both pp and Au+Au collisions, we construct a ratio known as the “nuclear modification factor”  $R_{AA}$ .

$$R_{AA}(p_T) = \frac{1/N d^2 N^{AA}/dp_T d\eta}{\langle N_{binary} \rangle d^2 N^{pp}/dp_T d\eta} \quad (1)$$

The number of binary collisions for a given centrality class  $\langle N_{binary} \rangle$  is estimated using a Glauber model of the nuclear overlap. In the (naive) limit that a nucleus-nucleus collision can be thought of as a superposition of independent nucleon-nucleon collisions, the nuclear modification factor at high  $p_T$  should be unity.

The measured nuclear modification factor is shown in Figure 2. There is a significant suppression of high transverse momentum  $\pi^0$  mesons observed in Au+Au collisions, consistent with substantial energy loss of the scattered partons [8]. A similar suppression was observed in data taken at  $\sqrt{s_{NN}} = 130$  GeV [9]. Models of energy loss that incorporate the expansion of the system indicate the energy loss in the matter created in heavy-ion collisions at RHIC may be as much as fifteen times larger than the energy loss of a comparable parton in ordinary nuclear matter [10]. Since the energy loss is proportional to the gluon density, this implies the gluon density created in a heavy ion collision is more than an order of magnitude larger than in cold nuclei.

## 5. Charm Production

The measurement of the production of charm is an exciting probe of heavy-ion collisions and a strong focus of the future of the PHENIX physics program. In particular, the production of charmonium bound states could be suppressed in the presence of a deconfined medium formed at RHIC [11], and such a signal has been suggested by data taken at the CERN SPS [12]. However, in order to characterize this suppression an overall knowledge of the total charm yield is required. PHENIX has made initial measurements in both of these areas.

### 5.1. Inclusive Electrons

The PHENIX collaboration has measured the production of single inclusive electrons and positrons from non-photonic sources using both a meson cocktail subtraction and special runs with a photon converter. The remaining  $e^+$  and  $e^-$  samples are candidates for electrons originating from the semileptonic decay of charm quarks. The transverse momentum distribution of electrons and positrons from non-photonic sources is shown

in Figure 3 for 10% central Au+Au collisions at  $\sqrt{s_{NN}} = 200$  GeV. The data is shown compared to a prediction from the event generator Pythia [13], which has been tuned to reproduce charm data from FNAL, the SPS and the ISR, scaled by the number of binary collisions for the 10% centrality class. Overall, the agreement is quite good, indicating there is neither a large enhancement or suppression of the production of charm quarks in these collisions.

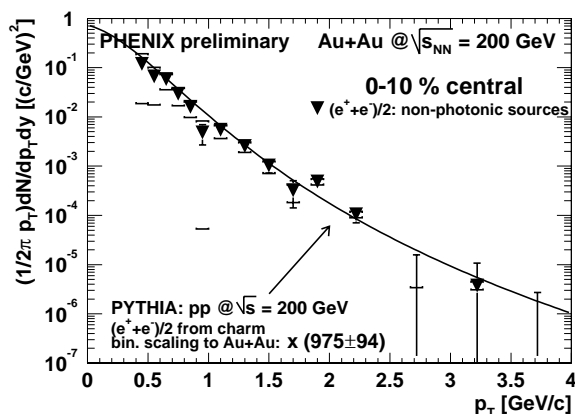


Figure 3. The transverse momentum distribution of single inclusive electrons and positrons for 10% central Au+Au collisions, shown compared to a Pythia prediction scaled by the appropriate number of binary collisions.

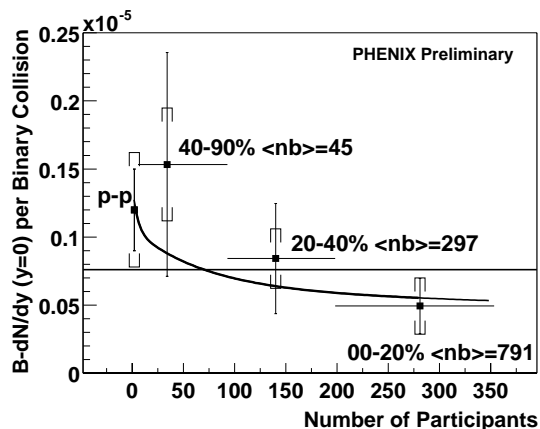


Figure 4. The  $J/\Psi \rightarrow e^+e^-$  branching ratio times the  $dN/dy$  measured in PHENIX and scaled by the number of binary collisions. The flat line indicates a best-fit binary scaling value, while the curve is the result of a nuclear absorption model assuming a 7.1 mb absorption cross section.

It is interesting to note that the results shown in Figure 5.1 may also indicate that heavy quarks may suffer a reduced energy loss in traversing the matter created during the collision.

## 5.2. $J/\Psi$ Production

As mentioned previously the production of charmonium has been proposed a signal for the production of a deconfined QCD medium in heavy-ion collisions [14]. PHENIX will measure  $J/\Psi$  production by the decay mode to two electrons in the central spectrometer arms, and by the decay to two muons using the two muon spectrometer arms. Preliminary data for the mode  $J/\Psi \rightarrow e^+e^-$  are shown in Figure 4. At the present time the uncertainties in the data are too large to allow discrimination between any but the most extreme scenarios. In future runs at RHIC, the PHENIX experiment will collect high statistics samples in both decay modes allowing a detailed study of charmonium production.

## 6. Summary and Outlook

The PHENIX experiment has embarked on a study of fundamental QCD using heavy-ion collisions at the Relativistic Heavy Ion Collider. A host of signals must be studied in detail and correlated before the existence of the QGP can be established. The study of hadronic observables, details of the early time behavior of the system from observables such as elliptic flow and jet quenching, as well as establishing the deconfined nature of the medium through such observables as charmonium suppression will be essential. In the next few years PHENIX will continue to pursue a physics program based on high statistics measurements of rare probes, combined with baseline measurements taken in p+p and d+Au collisions. This complete dataset will permit characterization of the matter created in heavy-ion collisions and further illuminate our understanding of fundamental QCD.

## REFERENCES

1. PHENIX Conceptual Design Report, BNL 1993 (unpublished), The PHENIX Collaboration, D. P. Morrison *et al.*, Nucl. Phys. **A638**, 565c (1998), and PHENIX Collaboration, Nucl. Inst. (submitted).
2. Harris J., Müller B. (1996) *Annu. Rev. Nucl. Part. Sci.* **46** p71.
3. K. Adcox *et. al.*, Phys. Rev. Lett **87**, 052301 (2001).
4. K. Adcox *et. al.*, Phys. Rev. Lett **88**, 242301 (2002).
5. PHENIX Collaboration, talk by T. Chujo *et. al.*, Proceedings of Quark Matter 2002, Nantes, to be published in Nucl. Phys. A.
6. M. Gyulassy, I. Vitev and X.-N. Wang, Phys. Rev. Lett. **86** 002537 (2001).
7. X.-N. Wang and M. Gyulassy, Phys. Rev. Lett. **68** 1480 (1992); M. Gyulassy and M. Plümer, Phys. Lett. **B243** 432 (1990).
8. PHENIX Collaboration, talk by S. Mioduszewski *et. al.*, Proceedings of Quark Matter 2002, Nantes, to be published in Nucl. Phys. A.
9. K. Adcox *et. al.*, Phys. Rev. Lett **88**, 022301 (2002).
10. E. Wang and X.-N. Wang, hep-ph/0202105.
11. for example, see R. Zhang *et. al.*, Phys. Rev. C **62**, 054905 (2000).
12. M. C. Abreu *et. al.* (NA50 Collaboration), Phys. Lett. **B521** 195 (2001).
13. T. Sjostrand *et. al.*, Comput. Phys. Comm. 135, 238 (2001).
14. T. Matsui and H. Satz, Phys. Lett. **B178**, 416 (1986).